# Continuous position measurements and the quantum Zeno effect

M. J. Gagen
*Department of Physics The University of Queensland Queensland 4072, Australia**

H. M. Wiseman and G. J. Milburn
*Department of Physics, The University of Queensland, Queensland 4072, Australia*
(Dated: July 1993)

We present a new model of continuous (in time) position measurements on a quantum system using a single pseudo-classical meter. The non-selective evolution of the system is described by a master equation which is identical to that obtained from previous models. The selective evolution is described by a stochastic nonlinear Schrödinger equation. The significance of this equation is that the stochastic term has a physical interpretation. By carefully choosing the parameters which define the meter and the system-meter coupling, we obtain a meter pointer with well-defined position which undergoes fluctuations. This 'jitter' in the pointer position gives rise to the stochastic dynamical collapse of the system wavefunction. By the inclusion of feedback on the meter, the pointer is made to relax towards an appropriate readout. We apply this model to the selective measurement of the position of a particle in a double well potential. In contrast to a recent claim [Phys. Rev. A, **46**, 1199 (1992)] we show that truly continuous position measurements lead to a quantum Zeno effect in certain parameter regimes. This is manifest by the changing of the particle dynamics from coherent tunnelling between the well minima to incoherent flipping, as in a random telegraph. As the measurement strength increases, the average length of time the particle remains stuck in one well increases proportionally.

## I. INTRODUCTION

The simplest model for position measurement is of course the projection postulate [1]. This is defined as follows (in one dimension for simplicity). A measurement of position $X$ of a particle at time $t$ has the result $X = x$ with probability $|\psi(x)|^2$, where $\psi(X)$ is the wavefunction of the particle in the position representation. Immediately after the measurement, the particle is in a position eigenstate with position probability distribution $\delta(X - x)$. This model of measurement is unrealistic for a number of reasons, the most important of which is that the projected system state has infinite energy. Also, it would desirable to have a model which would allow measurements continuous in time, as this allows the investigation of the so-called quantum Zeno effect [2–4]. This is the purely quantum phenomenon by which continuous measurement may arrest the evolution of the system.

A fruitful approach to develop more realistic measurement models is to expand the Hilbert space used to include a meter which is coupled to the particle. The meter is thus treated formally as a quantum mechanical system, but is expected to have some properties which makes it behave in a pseudo-classical manner. Of course, this does not solve the quantum measurement problem. It is still necessary to use the projection postulate on the meter. However, by moving this cut one step away from the system, we can hope for a more refined model. In the construction of our model, we were guided by three conditions which we believe apply to real laboratory meters: (a) the system interacts with a single meter over time, (b) the meter pointer is described by a continuous readout parameter, and (c) the system evolution is well-defined for any trajectory of the meter pointer.

The measurement model which we construct in Sec. II shares much in common with an earlier model of Caves and Milburn [5] and a similar approach by Lamb [6]. The most significant difference is that we have a single, well-defined pointer variable [as defined in conditions (a) and (b) above], rather than an succession of meters which are thrown away after each measurement. In the meter Hamiltonian we include a term, linear in the meter momentum, which shifts the pointer position. When the amount of the shift is made to depend on the results of measurement, this becomes a feedback stabilisation of the pointer. The nett effect is to cause the pointer to relax to a stable position determined by the measured system variable. Also, we derive an explicit stochastic Schrödinger equation for the wavefunction of the system conditioned on the meter readout. Similar differential equations have been proposed previously in the context of measurement theory [7–11]. However these have not been derived from a physical model for measurement involving a meter pointer, and hence the system wavefunction obeying these stochastic Schrödinger equations does not have a clear interpretation as a state conditioned on the meter readout.

In Sec. III, we apply the position measurement model to a simple and interesting case: a particle in a quartic double well potential. Of particular interest is how the measurement process disturbs the tunnelling of the low energy particle from one well to the other. We show that, in some experimental regimes, the quantum Zeno effect can be observed. This is manifest in the behaviour of the particle, which ceases to tunnel coherently between the wells, and instead flips incoherently between them in the manner of a random telegraph. The length of time the particle remains stuck in one well is proportional to the measurement strength. This result is in contrast to a recent claim by Fearn and Lamb [12] to the effect that there was no appearance of the quantum Zeno effect in the tunnelling behaviour of a particle in a double well system. As well as the full ponderomotive model, we consider the two-state approximation which is valid for particles with energy much lower than the barrier potential. The two states correspond to the particle localised

*Electronic address: m.gagen@imb.uq.edu.au

in the left or right well. This approximation is useful because the nonselective evolution is completely solvable, and the relation to the quantum Zeno effect has been studied in depth [13]. In addition, we take the opportunity to compare our measurement model with the two level example considered recently by Bonilla and Guinea [14].

The act of measuring the position of the particle causes its energy on average to increase linearly with time. The particle energy will eventually become greater than the potential barrier, and then the two-level approximation will cease to give insight into the behaviour of the system. The more accurate the measurement, the shorter the time over which the approximation will be valid. For weak measurements, this time may be much longer than the tunnelling time. For very strong measurements, there is no Zeno effect. Such measurements still cause the position variance of the wavepacket to be small, but the energetic wavepacket moves violently rather than being pinned to its starting point

## II. MODEL FOR CONTINUOUS SELECTIVE POSITION MEASUREMENTS

Consider a pseudo-classical meter with position and momentum operators $\hat{Q}$, and $\hat{P}$ respectively. We use the description pseudo-classical as we take the mass of the meter to infinity and the commutator $[\hat{Q}, \dot{\hat{Q}}] \to 0$. Thus the position of the meter, $X(t) = \langle \hat{Q} \rangle(t)$ is always well defined, as is its velocity. We describe the state of the meter by the ket $|X(t), P(t)\rangle$, which has the following form in the $Q$ representation ($\hat{Q}|Q\rangle = Q|Q\rangle$):

$$\langle Q|X(t),P(t)\rangle \;=\; (2\pi\sigma^2)^{-\frac{1}{4}} \exp\left\{-\frac{[Q-X(t)]^2}{4\sigma^2}\right\} \exp\left\{\frac{i}{\hbar}QP(t)\right\}. \tag{1}$$

Here, the spread in the position $\sigma$ will later be assumed to be arbitrarily small so that the meter wave function is well represented by its mean position $X(t)$. Throughout this paper we will generally be treating the state $|X(t), 0\rangle$. In this state, the meter has an average momentum of zero. Throughout this paper, the meter will be described by such a state. The meter moves only due to its interaction with the system, the Hamiltonian of which commutes with $\hat{P}$ and is subject to a frictional damping. We discuss how we achieve this below. Using these states is not essential, but does make the analysis simpler. The completeness relation for the states of the meter is therefore

$$\mathbf{I} \;=\; \int \frac{dX\, dP}{2\pi\hbar} |X,P\rangle\langle X,P|. \tag{2}$$

We will later require the inner product between two such states. This can readily be shown to be

$$C(X,Y) = \langle X,0|Y,0\rangle = \exp\left[-\frac{(X-Y)^2}{8\sigma^2}\right]. \tag{3}$$

We now turn our attention to the system, a particle with position operator $\hat{x}$. The system Hamiltonian $H_0$ is left arbitrary for the time being. The interaction between the system and the meter is of the form

$$\hat{H}_{SM} = \gamma \hat{P}[\hat{x} - F], \tag{4}$$

where $F$ is an arbitrary real number. In the case where $F = 0$ then this system-meter interaction is that considered by von Neumann [15] and later by Refs. [4, 5, 13]. This interaction translates the position of the meter by an amount proportional to the average position of the system. In the case where $F \neq 0$ then this term in the interaction causes a displacement of the meter coordinate. It has no effect on the dynamics of the system.

The state of the system-meter at time $t$ is taken to be

$$|\Phi(t)\rangle = |X(t), 0\rangle \otimes |\Psi(t)\rangle, \tag{5}$$

where $|\Psi(t)\rangle$ is a system ket. Then under the coupling of Eq. (4), and the free system Hamiltonian $H_0$, the combined state at time $t + \tau$ (for $\tau$ infinitesimal) is

$$|\Phi(t+\tau)\rangle \;=\; \exp\left\{-\frac{i\gamma\tau}{\hbar}\hat{P}\,[\hat{x}-F]\right\}|X(t),0\rangle \otimes|\Psi_0(t+\tau)\rangle_S, \tag{6}$$

where the state of the system at time $t + \tau$ is approximately

$$|\Psi_0(t+\tau)\rangle = (1 - \frac{i\tau}{\hbar}H_0)|\Psi(t)\rangle. \tag{7}$$

This evolution of the combined system-meter is purely unitary. The meter has undergone the desired translation due to the interaction with the system. The system has undergone its usual free evolution and has a measurement backaction operating on it due to the interaction with the meter.

Now since the meter is pseudo-classical it should always be describable by $X(t)$ with uncertainty $\sigma$. Its large mass ensures that it will be negligibly perturbed by a classical measurement process. Thus the effect of observing the meter state should be well modelled by a projection onto a new Gaussian state $|X(t+\tau), P(t+\tau)\rangle$. This step (using the projection postulate) is necessary at some stage in the measurement chain in order to describe the result of the measurement. The positioning of this formal procedure (the Heisenberg cut [16]) is essentially arbitrary, but the higher up the chain from the system to the observer the cut is placed the more accurate the model of the measurement will be. Placing the cut after the meter will yield a good description of the behaviour of the system and the meter.

The reasons we choose to project the meter onto a Gaussian state rather than an eigenstate of position as in previous models [5] are two fold. Firstly it is more realistic - creating a position eigenstate requires an infinite amount of energy. Secondly, we wish to use the meter again and so have it prepared in a Gaussian state as in the previous measurement period.

We note that using a Gaussian state with nonzero average momentum $P(t+\tau)$ will eventually modify the system dynamics and complicate the analysis. It is also our goal to model a meter pointer that is relatively stationary so as to enhance the accuracy of the readout. Such a model well represents the usual laboratory situation. This can be achieved by damping the momentum of the meter.

Following Caves and Milburn [5], this damping can be modelled by an instantaneous feedback term operating on the meter momentum. We apply a displacement operator $D[P(t+\tau)] = \exp(-iP(t+\tau)\hat{Q})$ to the readout meter state so that $D[P(t+\tau)]|X(t+\tau), P(t+\tau)\rangle = |X(t+\tau), 0\rangle$.

Following the projection and damping of the meter at time $t+\tau$ the state of the system-meter, given the readout result $X(t+\tau), P(t+\tau)$ is

$$\begin{aligned} |\Phi_c(t+\tau)\rangle &= P^{-1/2}(X,P)|X(t+\tau),0\rangle \\ &\quad \langle X(t+\tau), P(t+\tau)| \\ &\quad \exp\left\{-\frac{i\gamma\tau}{\hbar}\hat{P}\left[\hat{x}-F\right]\right\} \\ &\quad |X(t),0\rangle|\Psi_0(t+\tau)\rangle \\ &= P^{-1/2}(X,P)|X(t+\tau),0\rangle \otimes |\tilde{\Psi}_c(t+\tau)\rangle \end{aligned} \quad (8)$$

where we have defined an unnormalized system ket

$$\begin{aligned} |\tilde{\Psi}_c(t+\tau)\rangle &= \langle X(t+\tau), P(t+\tau)| \\ &\quad \exp\left\{-\frac{i\gamma\tau}{\hbar}\hat{P}\left[\hat{x}-F\right]\right\} \\ &\quad |X(t),0\rangle|\Psi_0(t+\tau)\rangle, \end{aligned} \quad (9)$$

Here we use the subscript $c$ to indicate that the state of the system is conditioned on the previous readout variable $X(t)$. That is, we are considering selective evolution of the system, hence the possibility of using a wavefunction rather than a density operator description.

The normalization term $P(X,P)$ is equal to the probability of obtaining the result $X(t+\tau), P(t+\tau)$ and is given by

$$P(X,P) = \langle\tilde{\Psi}_c(t+\tau)|\tilde{\Psi}_c(t+\tau)\rangle. \quad (10)$$

However, after setting the meter momentum to zero we are not interested in the readout $P(t+\tau)$, but only in the meter position $X(t+\tau)$. The probability to obtain a reading $X(t+\tau)$ is $P(X)$ and is given by

$$\begin{aligned} P(X) &= \int dP\ P(X,P) \\ &= \mathrm{tr}\left(\ \hat{\rho}_0(t+\tau)\times\right. \\ &\quad \left.|\ C(X(t+\tau), X(t)+\gamma\tau[\hat{x}-F])\ |^2\ \right), \end{aligned} \quad (11)$$

where we write $\hat{\rho}_0(t+\tau) = |\Psi_0(t+\tau)\rangle\langle\Psi_0(t+\tau)|$. In this equation we have resolved the exponential as a translation of the meter, and made use of Eq. (3). We note that $P(X)$ is given in terms of states with zero average momentum as the displacement operator $D[P(t+\tau)]$ translates the meter state without changing the projection onto the $\hat{Q}$ axis.

The mean and variance for the distribution of $X(t+\tau)$ are

$$\langle X(t+\tau)\rangle = X(t) + \gamma\tau[\langle\hat{x}\rangle_c - F] \quad (12)$$

$$V(X(t+\tau)) = 2\sigma^2 + \gamma^2\tau^2 V(\hat{x}). \quad (13)$$

In order to obtain smooth evolution of the *system*, we will show shortly that the following measurement parameter must be finite in the limit $\tau \to 0$:

$$\Gamma = \frac{\gamma^2\tau}{8\sigma^2}. \quad (14)$$

| n | $\sigma \sim \tau^n$ | $\gamma \sim \tau^{n-1/2}$ | $\dot{X}(t) \sim \tau^{n-1/2}$ |
|---|---|---|---|
| $\frac{1}{2}$ | $\sqrt{\tau}$ | 1 | Well Defined |
| $-\frac{1}{2}$ | $1/\sqrt{\tau}$ | $1/\tau$ | Not Defined |

TABLE I: *A finite parameter $\Gamma = \gamma^2\tau/8\sigma^2$ in the limit $\tau \to 0$ gives smooth system evolution. Whether this also gives smooth evolution of the meter pointer $X(t)$ depends on how $\gamma$ and $\sigma$ are scaled. The scaling can be defined by a real parameter $n$. Two scalings of interest are given, the first being that used in this paper and the second corresponding to the model of Caves and Milburn [5]*

The implications of this for the *meter* evolution is that in Eq. (13), the $2\sigma^2$ term will dominate in the limit $\tau \to 0$. In this case $X(t+\tau)$ is well approximated by a Gaussian random variable, and can be replaced by

$$X(t+\tau) = X(t) + \gamma\tau\left(\langle\hat{x}\rangle_c(t) - F + \frac{1}{2\sqrt{\Gamma}}\xi(t)\right), \quad (15)$$

where $\xi(t)$ indicates Gaussian noise of standard deviation $1/\sqrt{\tau}$. Since this term is independent from one $\tau$ increment to the next, in the limit $\tau \to 0$ it can be modelled by white noise $\xi(t)$ with $\langle\xi(t)\xi(t')\rangle = \delta(t-t')$. Note that $F$, which we have so far left arbitrary, can be chosen to be a function of $X(t)$, the previous measurement result. This allows feedback on the meter position to prevent the meter pointer from becoming unbounded, which was an undesirable feature of previous models [5].

It is evident that Eq. (15) describes a driven meter with position diffusion, providing that $\gamma$ is finite as $\tau \to 0$. This is a natural choice as we wish to follow the dynamics of the meter pointer. However, it is not a necessary assumption. The choice of scaling of $\gamma$ fixes the scaling of $\sigma$ if $\Gamma$ is to remain finite. The various possibilities can be labelled by a real number $n$, as shown in Table I.

Our choice corresponds to $n = 1/2$, in which the position uncertainty of the meter goes to zero with $\tau$. This is consistent with our earlier statement that the position of the meter is defined arbitrarily accurately.

Taking the limit $\tau \to 0$ in Eq. (15), we see that the meter position $X(t)$ obeys the following stochastic differential equation

$$\dot{X}(t) = \gamma\left[\langle\hat{x}\rangle_c(t) - F + \frac{1}{2\sqrt{\Gamma}}\xi(t)\right]. \quad (16)$$

Here the effect of the feedback term $F$ is evident. In this paper we take $F = X(t)$ and this corresponds to the meter pointer relaxing at rate $\gamma$ to the conditioned system mean $\langle\hat{x}\rangle_c(t)$. This is the motivation for the original Hamiltonian coupling between the meter and the system: it allows the position of the system to be read (however inaccurately) from the position of the meter pointer. Previous models [5] have treated the case where $F = 0$, whereby the information about the system operator of interest is encoded in the *velocity* of the meter pointer, and an experimenter would have to extract this information explicitly. The choice of the function $F$ has no effect on the system dynamics.

In addition to relaxing towards its appropriate value, the meter pointer undergoes a 'jitter' due to the noise term $\xi(t)$ in Eq. (16). The size of this jitter can be made small by taking the limit $\gamma \ll \Gamma$. However, as we

will show [Eq. (21)], this would mean that the system would collapse towards a position eigenstate on a time scale $\Gamma^{-1}$ much faster than the time scale $\gamma^{-1}$ on which the meter could respond. There is thus an obvious trade off between the jitter and the response of the meter.

We return now to the evolution of the system, conditioned on the meter readout $X(t)$. From Eq. (8), the combined state of the system and meter at time $t+\tau$ is a decoupled one, as it was at time $t$. We can thus write the new conditioned system state at time $t+\tau$, after discarding the result $P(t+\tau)$ as

$$|\Psi_c(t+\tau)\rangle = P^{-1/2}(X)|\tilde{\Psi}_c(t+\tau)\rangle, \tag{17}$$

where the unnormalized ket $|\tilde{\Psi}_c(t+\tau)\rangle$ is defined in Eq. (9).

This result can be simplified by substituting for the meter evolution [Eq. (15)] and using Eq. (3) to evaluate the inner product in Eq. (11). This gives

$$\begin{aligned} |\Psi_c(t+\tau)\rangle &= P^{-1/2}(X)e^{-\Gamma\tau[\hat{x}-\langle\hat{x}\rangle_c-\frac{1}{2\sqrt{\Gamma}}\xi(t)]^2} \\ &\quad |\Psi_0(t+\tau)\rangle. \end{aligned} \tag{18}$$

As we have obtained an exponential that is first order in $\tau$ we can obtain a stochastic differential equation for the evolution of the system. When we expand the exponential (carefully because of the noise term) we obtain

$$\begin{aligned} \tfrac{d}{dt}|\Psi_c(t)\rangle &= \left(-\frac{i}{\hbar}H_0 - \frac{\Gamma}{2}[\hat{x}-\langle\hat{x}\rangle_c]^2\right. \\ &\quad \left.+\sqrt{\Gamma}\xi(t)[\hat{x}-\langle\hat{x}\rangle_c]\right)|\Psi_c(t)\rangle. \end{aligned} \tag{19}$$

It is interesting to note that this stochastic Schrödinger equation is identical to that resulting from homodyne detection [17] with the replacement $\hat{a}\to\hat{x}$. Similar equations have also been considered in Ref. [7–11, 18, 19]. The significance of the approach considered here is that we have an unravelling of the master equation as an ensemble of stochastic, continuous trajectories for the state vector of the system. Each of these trajectories has an explicit interpretation in terms of the readout of a continuous pseudo-classical meter. This we believe to be a new feature that may have important applications.

Later in this paper, we will be comparing our model with that proposed by Bonilla *et.al.* [14]. The advantage of our model is that the collapse of the system wave function is a natural outcome of the measurement process, as might be expected. This is in contrast to their approach where a system-environment interaction is introduced in order to achieve a collapse to an eigenstate of the measured quantity. Also, their model does not guarantee correct measurement statistics. That our model does guarantee this is evident from the nonselective master equation (21) which we derive below. If the free evolution from $H_0$ can be ignored, then the statistics of the measured quantity $\hat{x}$ remains unchanged. Since an eigenestate of $\hat{x}$ is also an eigenstate of the stochastic evolution generator [Eq. (19)], again ignoring $H_0$, this shows that the system will end up in an eigenstate with the appropriate probability. It is when $H_0$ cannot be ignored that the superiority of our model over the projection postulate emerges.

The stochastic Schrödinger equation (19) is easily shown to be equivalent to the following stochastic master equation for the selective evolution of the conditioned density operator:

$$\begin{aligned} \dot{\rho}_c(t) &= \frac{-i}{\hbar}[H_0,\rho_c] - \frac{\Gamma}{2}[\hat{x},[\hat{x},\rho_c]] \\ &\quad +\sqrt{\Gamma}\xi(t)\left(\hat{x}\rho_c + \rho_c\hat{x} - 2\langle\hat{x}\rangle_c\rho_c\right). \end{aligned} \tag{20}$$

This stochastic master equation is conditioned on the entire history of the meter readout $X(t)$. If we were only interested in the non-selective evolution of the system, then we would have to discard all knowledge of the evolution of the system. This is achieved in the usual manner of averaging over all possible meter readouts at all times $t$. In our case this simply amounts to averaging over the stochastic term in Eq. (20), which gives zero since $\xi(t)$ is independent of the system state at time $t$. The nonselective master equation for the system is thus

$$\dot{\rho}_{NS}(t) = \frac{-i}{\hbar}[H_0,\rho_{NS}] - \frac{\Gamma}{2}\left[\hat{x},[\hat{x},\rho_{NS}]\right]. \tag{21}$$

This is the expected double-commutator form of the non-selective master equation which usually arises from system-meter couplings which do not disturb the measured quantity such as that employed in Eq. (4).

If $H_0$ can be written as

$$H_0 = \frac{\hat{p}^2}{2m} + V(\hat{x}), \tag{22}$$

then the nonselective master equation (21) yields

$$\frac{d}{dt}\langle\hat{x}\rangle = \frac{1}{m}\langle\hat{p}\rangle \tag{23}$$

$$\frac{d}{dt}\langle\hat{p}\rangle = -\langle V'(\hat{x})\rangle. \tag{24}$$

That is to say, the measurement term does not affect the Ehrenfest relations. If $V$ is a polynomial up to second order in $\hat{x}$, then these equations are closed. Thus the measurement has no effect on the mean value of $\hat{x}$ if the particle moves in a linear or quadratic potential. This means for example that no Zeno effect could be manifest in such systems. In the following section we examine motion in a quartic potential. It can be shown that the effect of the measurement first appears with the fifth order derivative

$$\frac{d^5}{dt^5}\langle\hat{x}\rangle \sim -24c\Gamma\langle\hat{x}\rangle, \tag{25}$$

where $c$ is the coefficient of $\hat{x}^4$ in $V(\hat{x})$.

## III. TUNNELLING IN A DOUBLE WELL POTENTIAL

In this section we apply our model to the measurement of the position of a particle in a double well potential. We demonstrate the measurement regimes in which the quantum Zeno effect will be apparent.

The Hamiltonian for a particle in a quartic double well potential is

$$H_0 = \frac{\hat{p}^2}{2m} - \frac{m\omega_0^2}{4}\hat{x}^2 + \frac{m^2\omega_0^4}{64D}\hat{x}^4, \tag{26}$$

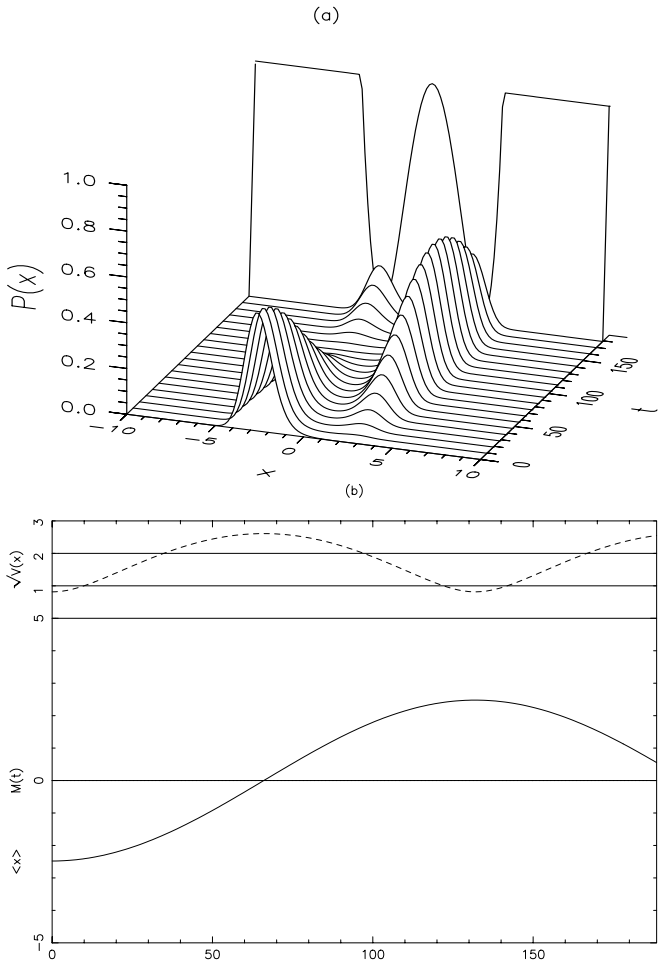


FIG. 1: Free Evolution with $\Gamma = 0$. (a) Plot of the time evolution of probability density for the system position $\hat{x}$ of a particle undergoing free evolution in a double well potential (shown at rear of plot). With $\Gamma = 0$, the particle coherently tunnels from the left to the right well. (b) Plot the time evolution of the average position of the particle $\langle \hat{x} \rangle_c$ (heavy line) and the position standard deviation $V(x)$ (dashed line) for the same value of $\Gamma$ as in (a).

where $m$ is the mass of the particle, $D$ is the height of the potential barrier between the minima and $\omega_0$ is the frequency of oscillation of the particle in one of the minima (approximated as a quadratic potential). Such a double well system has been extensively studied (see Refs. [20, 21] and references therein). We transform to natural units by setting $m = \hbar = \omega_0 = 1$. We obtain for the Hamiltonian

$$H_0 = \frac{1}{2}\hat{p}^2 - \frac{1}{4}\hat{x}^2 + \beta \hat{x}^4, \tag{27}$$

where $\beta = 1/(64D)$ and $D$ is now dimensionless.

The double well potential has alternating odd and even eigenstates. Those with energies well below the barrier potential will be nearly degenerate in pairs, and superposition of these pairs can be constructed so as to give states well localised in the left or the right well. Such states will be like coherent states of a harmonic oscillator centred on the minima of the respective wells. In this paper we set the depth $D = 1$, which has the eigenvalue structure for the double well shown in Table II.

We consider the first two such localised states, $|+\rangle$, and $|-\rangle$, found in the right and left hand wells respectively.

| $\|i\rangle$ | $E_i$ | $\Delta$ | $T_t$ |
|---|---|---|---|
| $\|1\rangle$ | -0.54980 | 0.023923 | 131.32 |
| $\|2\rangle$ | -0.52587 | | |
| $\|3\rangle$ | 0.09262 | | |
| $\|4\rangle$ | 0.39333 | | |

TABLE II: *The eigenvalue structure of the double well treated in this paper with depth $D = 1$. Also shown is the energy difference between the bottom pair of states $\Delta$ and the associated tunnelling time $T_t$.*

These states are given by

$$|\pm\rangle = \frac{1}{\sqrt{2}}\left(|1\rangle \pm |2\rangle\right). \tag{28}$$

We choose as our initial state $|-\rangle$ and monitor the time the particle takes to tunnel to the right hand well when its state is $|+\rangle$. This tunnelling occurs under free evolution, and the time taken $T_t$ is given by the inverse energy difference between the states $|1\rangle$ and $|2\rangle$

$$T_t = \frac{\pi}{\Delta}. \tag{29}$$

We see this tunnelling behaviour clearly in Fig. 1(a). Here we show the evolution of the probability density for the system position $\hat{x}$ under free evolution. With purely unitary evolution, the system is completely equivalent to a two-level system, because of the chosen initial conditions. In Fig. 1(b) we show the time evolution of the average position of the particle and the position standard deviation. The numerical technique we used to simulate the behaviour of the particle in the double well potential is described in App. A.

### A. Numerical Solution of exact system

It is obvious that vanishingly weak measurements ($\Gamma \to 0$) will not manifest the quantum Zeno effect. In this limit there is no measurement backaction on the system. However, it is also the case for the system considered here that too strong a measurement process also makes the quantum Zeno effect unobservable. This arises as the measurement backaction on the system tends to increase the particles energy. A highly energetic particle will not tunnel through the middle barrier; rather it will pass over it. If we wish to observe the quantum Zeno effect, we must limit the measurement backaction on the system.

The measurement regime to demonstrate the Zeno effect can be established by considering a non-selective measurement process. At any time the average energy of the particle is given by Eqs. (21) and (27) as

$$\begin{aligned} \dot{E}_{NS} &= \mathrm{tr}(H_0 \dot{\hat{\rho}}_{NS}) \\ &= \frac{\Gamma}{2}. \end{aligned} \tag{30}$$

With the initial condition $E_{NS}(0) = E_- = (E_1 + E_2)/2$ we then have

$$E_{NS}(t) = E_- + \frac{\Gamma}{2}t. \tag{31}$$

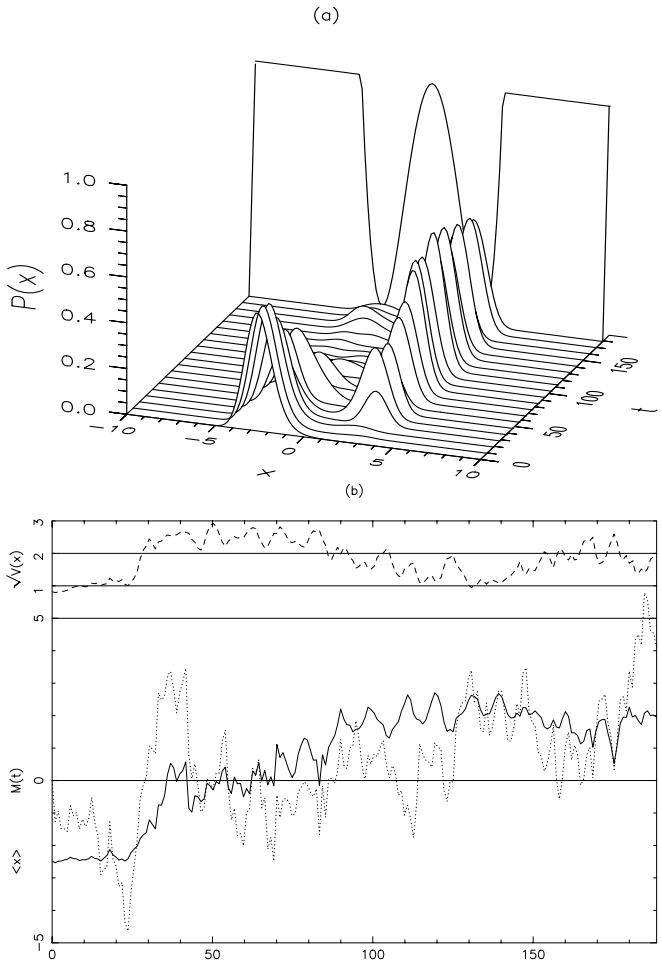


FIG. 2: Random Walk regime with $\Gamma = 0.001$. (a) As in Fig. 1(a), with $\Gamma = 0.001$. The coherent tunnelling has a "random walk" added. (b) As in Fig. 1(b). The meter readout is shown by a dotted line. Since $\gamma = 0.05$, the "jitter" in the meter is large.

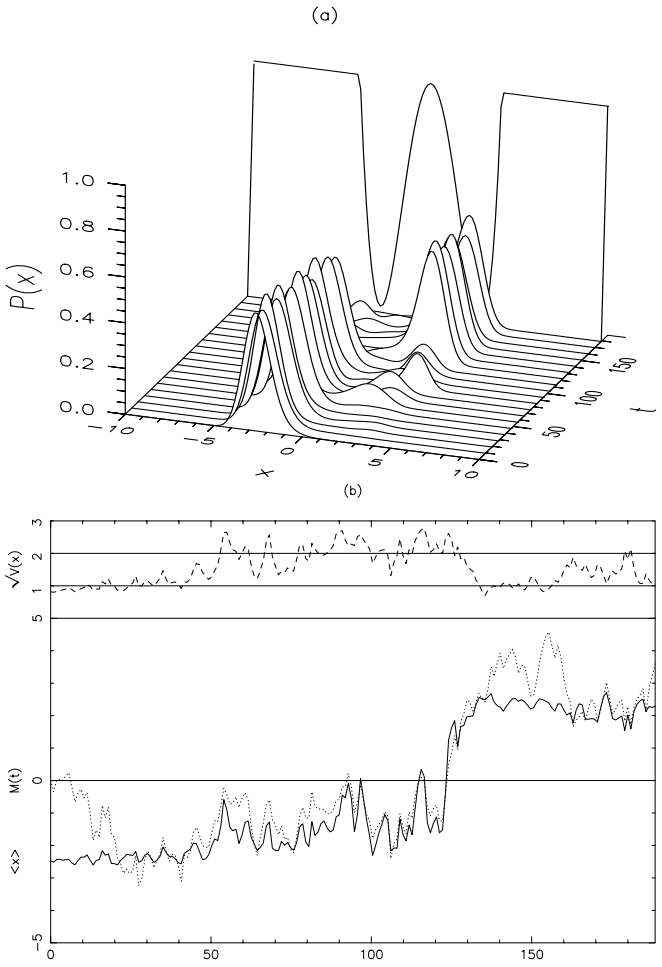


FIG. 3: Random Telegraph regime with $\Gamma = 0.003$. (a) As above with $\Gamma = 0.003$. The particle undergoes a random telegraph type evolution from one minima to the other. (b) As above.

In this paper we wish to observe tunnelling behaviour on a time scale of about one tunnelling time $T_t$. For the double well system we are using (see Table II) tunnelling will occur as long as we do not excite level $|3\rangle$. We require that $E_{NS}(T_t) \ll E_3$. This constraint gives

$$\Gamma \ll \frac{2}{T_t}(E_3 - E_-) \sim \Delta. \tag{32}$$

We see that the measurement strength must scale inversely with the time over which we wish to see tunnelling behaviour. Of course, any measurement interaction with $\Gamma > 0$ will eventually excite the particle enough to leave the tunnelling regime. Once the particle is sufficiently energetic, the quantum Zeno effect will not be observable.

From the two level approximation in the next section, it can be shown that the Zeno effect will exist only for

$$\Gamma \gtrsim \frac{\Delta}{8D}. \tag{33}$$

The two level approximation is strictly only valid for $D \gg 1$. There is thus a parameter region where the Zeno effect may appear : $\Delta/8D \lesssim \Gamma \ll \Delta$. For the well considered in this paper ($D = 1$), we require $0.003 \lesssim \Gamma \ll 0.01$. This window is rather narrow but is nevertheless present as our numerical results show. As $D \to \infty$, the Zeno effect would be manifest over a large range of measurement parameter $\Gamma$. The reason that we use $D = 1$ rather than $D \gg 1$ as would be desirable is that the tunnelling time increases like $\exp(16D/3)$ for large $D$ [22], which would make numerical simulations prohibitively time consuming.

The selective evolution of the particle wavefunction under position measurements is given by Eq. (19) with $H_0$ given by Eq. (27). We gradually increase the effectiveness of our measurement, and plot typical trajectories. In each of these figures we show (a) a plot of the probability density for the position of the particle, and (b) the average position of the particle (heavy line), the readout meter variable (dotted line) and the standard deviation in the position of the particle (dashed line). The readout meter parameters have been set fixed with $\gamma = 0.05$ and $F = X(t)$. (See App. A for details of the numerical method used.)

In Fig. 2, $\Gamma = 0.001$ and the particle undergoes a diffusive random walk. This is seen most clearly in the average position evolution. The "walk" is dominated by the free unitary evolution. We note the large scale of the "jitter" in the meter readout in Fig. 2(b). With the chosen meter parameters the meter response [determined by $\gamma/\sqrt{\Gamma}$ in Eq. (16)] is too large. The response improves

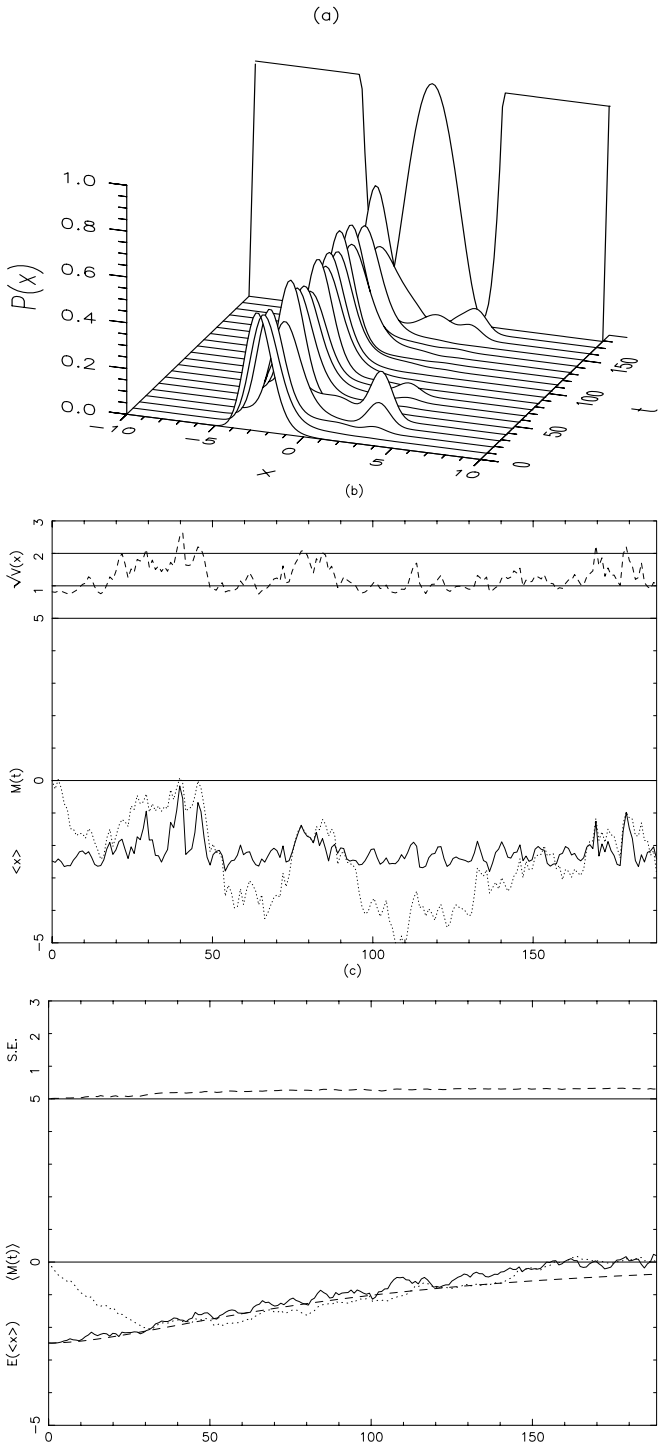


FIG. 4: The quantum Zeno effect with $\Gamma = 0.005$. (a) As above with $\Gamma = 0.005$. We see strong evidence of the quantum Zeno effect in the delayed transition from the left to the right well. The particle position is somewhat squeezed. (b) As above. (c)Plot of the ensemble average evolution of the meter position (dotted line) and the (quantum) mean particle position (solid line). These nonselective averages were calculated using an ensemble of 40 selective runs. The Standard Error (S.E.) in the mean particle position is also shown. This clearly shows that the free evolution of the particle has been arrested in the manner of a Zeno effect and is in good agreement for short times with the theoretical curve for the nonselective particle position calculated using the two level approximation (dashed curve).

in later figures as $\Gamma$ increases.

The transition to the random telegraph regime is seen very clearly in Fig. 3 where $\Gamma = 0.003$. The particle is trapped for some considerable time in the left well, and then makes a random, and sudden transition to the right hand well.

In Fig. 4 we are well into the regime where we manifest the quantum Zeno effect with $\Gamma = 0.005$. The behaviour is fully described by a random telegraph. Further, the survival probability of the particle in the initial state is significantly enhanced. During the time of observation, the particle did not jump to the right well. This is the quantum Zeno effect. Finally we discern some squeezing in the particle's position probability density under this level of selective measurement. The squeezed particle is more energetic, and we anticipate that our two level approximation will break down and the quantum Zeno effect cease for stronger measurements.

In addition to the typical selective trajectory, we include in Fig. 4(c) the ensemble average evolution of the meter position and the (quantum) mean particle position. These nonselective averages were calculated using an ensemble of 40 selective runs. The results clearly show that the free evolution of the particle has been arrested in the manner of a Zeno effect. We also include a theoretical curve for the nonselective particle position. This was calculated using the two level theory of the next section, but with the replacement of $\sqrt{8D}$ by 2.48, as the latter is a better approximation to the position of the particle when it is localised in one of the wells. It is clear that the theoretical curve is in good agreement with the numerical results (within the standard error due to the finite size of the ensemble), at least for times less than the free tunnelling time $T_t \simeq 131$. This is not unexpected, as we know that the two level approximation breaks down for times greater than $T_t$.

The complete breakdown of the two level approximation is confirmed in Fig. 5, where $\Gamma = 0.01$. The particle is very energetic and is no longer trapped at the bottom of either of the minima. The backaction of the strong selective measurements is such that the particle has left the two-level regime and is energetically oscillating across the entire width of the double well potential. In a single tunnelling time $T_t$ the particle can be found any number of times on the left or the right hand side of the double well potential. The quantum Zeno effect can no longer be observed.

The behaviour seen in this last plot is similar to that observed in the results of Fearn and Lamb [12]. We believe that herein lies part of the explanation as to why they failed to observe the quantum Zeno effect. Their measurement parameters were apparently chosen so that their particle became highly energetic very quickly, and so could not remain trapped in one well. In addition, their measurement model, unlike ours, does not correspond to strictly continuous measurements, as required to see the Zeno effect. We have demonstrated that a realistic model for continuous position measurements of a particle does result in the Zeno effect in at least some experiments.

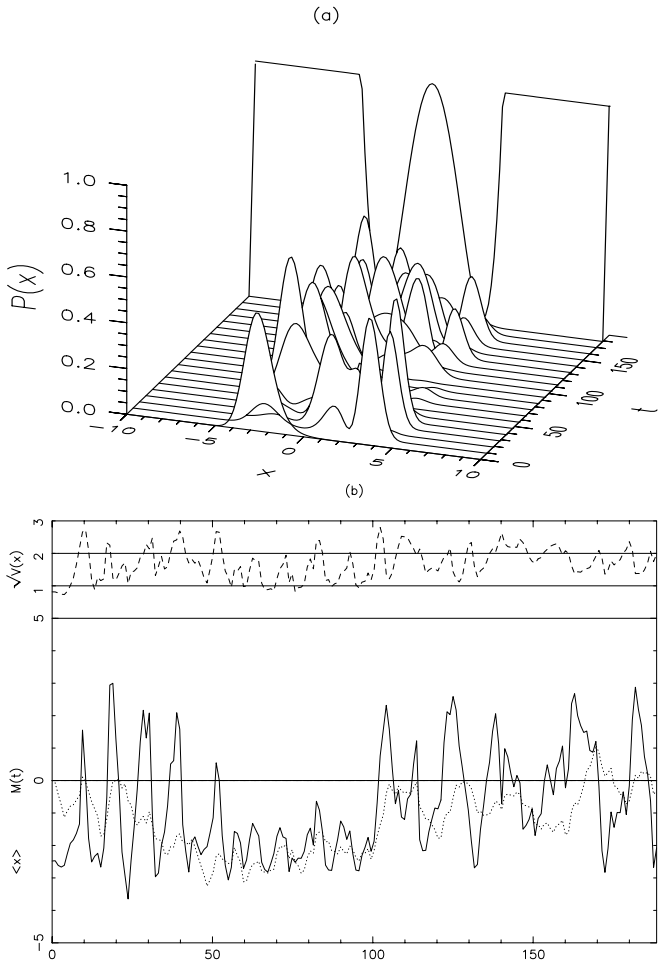


FIG. 5: The energetic particle evolution with $\Gamma = 0.01$. (a) As above with $\Gamma = 0.01$. The particle is very energetic and is no longer trapped at the bottom of either of the minima. The measurement backaction is so strong that the particle has left the regime of the two level approximation, so we don't expect the Zeno effect to be manifest. (b) As above. The particle is energetically oscillating across the entire width of the double well potential. In this plot the particle can be found a number of times on the left or the right hand side of the double well potential. Note that the meter is lagging behind the higher frequency oscillations.

### B. The two level approximation

We have previously commented on the similarity of the free evolution tunnelling behaviour of the particle to that of coherent evolution of a driven two level system (see Refs. [20, 21]). This approximation is explored in this section. Our two level treatment has the additional advantage of allowing us to compare our measurement model directly to that considered by Bonilla and Guinea [14].

As previously indicated, we are able use an approximate discrete two-level basis for a particle in the double well potential provided that it has sufficiently low energy so that the occupation of the energy eigenstates is restricted to the lowest two states. This approximation effectively converts the position operator into a discrete operator with eigenvalues "left" and "right". In this pseudo-discrete system, the quantum Zeno effect can be readily manifest.

In the two level approximation, we use only the states $|1\rangle, |2\rangle$ or equivalently, $|+\rangle, |-\rangle$. It can readily be shown that the free Hamiltonian of the double well is equivalent to

$$\begin{aligned} H_0 &= \frac{\Delta}{2}\begin{pmatrix} -1 & 0 \\ 0 & 1 \end{pmatrix}_{1,2} \\ &= -\frac{\Delta}{2}\begin{pmatrix} 0 & 1 \\ 1 & 0 \end{pmatrix}_{\pm} \\ &= -\Delta\hat{\sigma}_x. \end{aligned} \tag{34}$$

Here we use the usual Pauli matrices $\hat{\sigma}_x, \hat{\sigma}_y, \hat{\sigma}_z$ as operators in the $|\pm\rangle$ basis. The position measurement operator is

$$\begin{aligned} \hat{x} &= \sum_{i,j=1}^{\infty} \langle j|\hat{x}|i\rangle \ |i\rangle\langle j| \\ &\approx \sum_{i,j=1}^{2} \langle j|\hat{x}|i\rangle \ |i\rangle\langle j| \\ &= \langle 1|\hat{x}|2\rangle \ |2\rangle\langle 1| + \text{H.c.}, \end{aligned} \tag{35}$$

where H.c. means the Hermitian conjugate. In deriving the above we have made the two level approximation and used the evenness and oddness of the eigenstates of the Hamiltonian. Given this approximation we readily show that

$$\begin{aligned} \hat{x} &\approx \sqrt{8D}\begin{pmatrix} -1 & 0 \\ 0 & 1 \end{pmatrix}_{\pm} \\ &= 2\sqrt{8D}\,\hat{\sigma}_z. \end{aligned} \tag{36}$$

Here $\pm\sqrt{8D}$ are the positions of the double well minima, which for $D \gg 1$ are very close to the mean positions of the left and right wavefunctions.

We are interested in following the selective evolution of the particle under position measurements, and also the non-selective evolution when no account is taken of the measurement results. For convenience we rewrite the relevant evolution equations for the two level approximation for the double well system. The stochastic Schrödinger equation for the selective evolution of the state vector is

$$\begin{aligned} \tfrac{d}{dt}|\Psi_c(t)\rangle &= ( \ i\Delta\hat{\sigma}_x - 16D\Gamma[\hat{\sigma}_z - \langle\hat{\sigma}_z\rangle_c]^2 \\ &\quad +4\sqrt{2D\Gamma}\xi(t)[\hat{\sigma}_z - \langle\hat{\sigma}_z\rangle_c] \ )\,|\Psi_c(t)\rangle. \end{aligned} \tag{37}$$

The non-selective master equation for the two level system is

$$\dot{\rho}_{NS}(t) = i\Delta[\hat{\sigma}_x, \rho_{NS}] - 16D\Gamma\,[\hat{\sigma}_z, [\hat{\sigma}_z, \rho_{NS}]]\,. \tag{38}$$

First we consider the selective evolution of our two level tunnelling system. We define the components of the Bloch vector as

$$\begin{aligned} X(t) &= \langle\hat{\sigma}_x(t)\rangle \\ Y(t) &= \langle\hat{\sigma}_y(t)\rangle \\ Z(t) &= \langle\hat{\sigma}_z(t)\rangle. \end{aligned} \tag{39}$$

The evolution of the Bloch vector is readily shown to be

$$\tfrac{d}{dt}\begin{pmatrix} X \\ Y \\ Z \end{pmatrix} = \begin{pmatrix} -16D\Gamma & 0 & 0 \\ 0 & -16D\Gamma & \Delta \\ 0 & -\Delta & 0 \end{pmatrix}\begin{pmatrix} X \\ Y \\ Z \end{pmatrix}$$

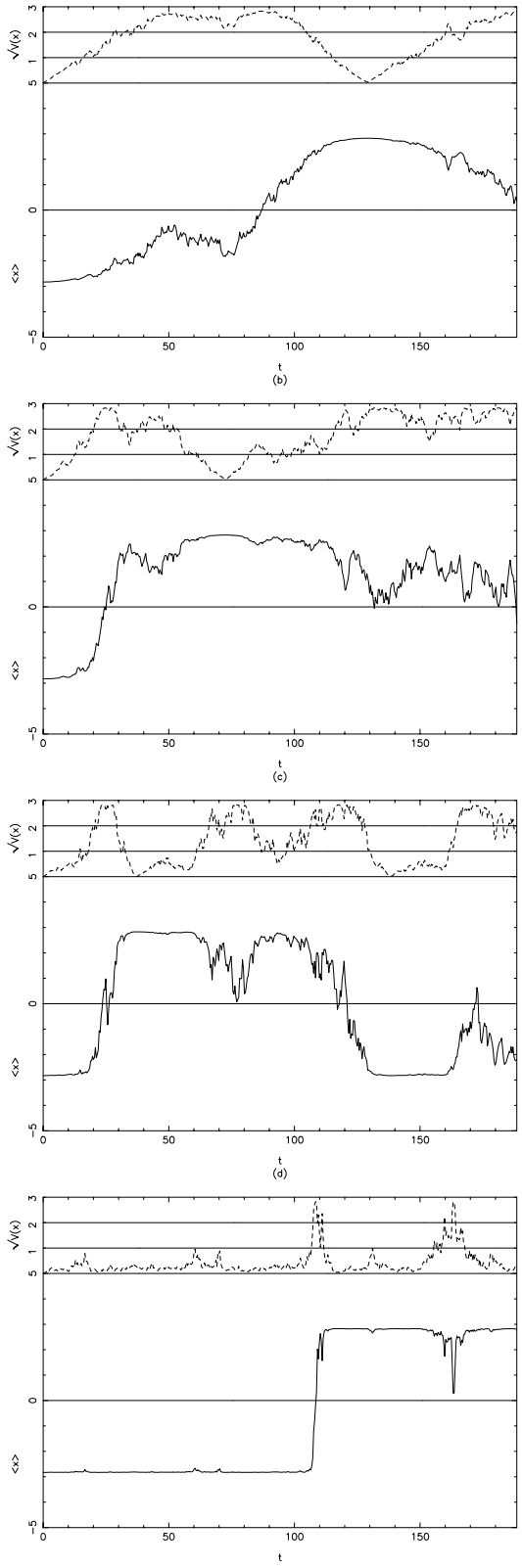


FIG. 6: The two level approximation. Plot of typical selective evolution of the mean and standard deviation of the position of a continuously monitored particle under the two level approximation. (a) For $\Gamma \approx 0$ the particle tunnels almost unitarily from one minima to the other. (b) For $\Gamma = 0.0003$, some "random walking" is seen but the particle's motion is still largely dominated by the unitary terms. As $\Gamma$ increases [(c) $\Gamma = 0.003$ and (d) $\Gamma = 0.01$] the behaviour of the particle changes to a "random telegraph" type evolution. The quantum Zeno effect is evident in the enhanced trapping of the particle in the left well for large $\Gamma$.

$$+ \; 8\sqrt{2D\Gamma}\xi(t) \begin{pmatrix} -XZ \\ -YZ \\ \frac{1}{4} - Z^2 \end{pmatrix}. \qquad (40)$$

This equation has no stable points for the case where $\Delta, \Gamma > 0$. However, we gain an understanding of the dynamics by considering each term separately. As for the non-selective case, the deterministic term has stable point $X = Y = Z = 0$, representing a fully mixed state. In contrast, the noise term has stable point $X = Y = 0, Z = \pm 1/2$. These points correspond to the two eigenstates $|\pm\rangle$ so it is evident that the measurement term encourages collapse to one of the two eigenstates of the measurement operator.

Herein lies the clearest statement of the difference between our model and that considered in Ref. [14]. [The above equation for the dynamics of the Bloch vector compares directly to their Eq. (3.9).] Our model incorporates the collapse of the wave function in a natural way as a direct outcome of the interaction between a pseudo-classical meter and the system of interest. Also the fact that our nonselective master equation preserves the probability distribution for $\hat{\sigma}_z$ ensures that the system tends towards each eigenvalue with the correct probability, unlike the model of Bonilla and Guinea [14].

In Fig. 6 we show typical trajectories of the system with various measurement strengths $\Gamma$. Specifically, we show the mean and variance of the position of the particle (which is given by the $Z$ component of the Bloch vector). These trajectories show a strong similarity to those found from the full ponderomotive model. For $\Gamma = 0$ we see the unitary evolution of the particle as it tunnels from one minima to the other. For $\Gamma = 0.0003$ we still see tunnelling due to the unitary evolution, but there is some noise superimposed, especially around the time when the particle is not localised in either well. As $\Gamma$ increases we discern a gradual elimination of the unitary evolution. For large $\Gamma$ the particle undergoes a "random telegraph" type evolution. The quantum Zeno effect is evident in the enhanced time of trapping of the particle in the left well for large $\Gamma$.

We now turn our attention to the deterministic terms in this stochastic equation. These terms are those resulting from the non-selective evolution in Eq. (38). The evolution of this two level system in the non-selective case has been extensively studied [13]. With an initial state $|-\rangle$ ($X(0) = Y(0) = 0, Z(0) = -1/2$), the general solution is

$$\begin{aligned} X(t) &= 0 \\ Y(t) &= -\frac{\Delta}{2\Omega} e^{-8D\Gamma t} S(\Omega t) \\ Z(t) &= -\frac{1}{2\Omega} e^{-8D\Gamma t} \left[ 8D\Gamma S(\Omega t) + \Omega C(\Omega t) \right], \end{aligned} \qquad (41)$$

where we have $\Omega = \sqrt{|(8D\Gamma)^2 - \Delta^2|}$ and for $8D\Gamma < \Delta$ we set $S(\Omega t) = \sin \Omega t, C(\Omega t) = \cos \Omega t$ and for $8D\Gamma > \Delta$ we set $S(\Omega t) = \sinh \Omega t, C(\Omega t) = \cosh \Omega t$.

This nonselective evolution is shown in Fig. 7. We plot the non-selective evolution of the average value of $\langle \hat{x} \rangle$ for a particle initially well localised in the left well. We vary the measurement parameter $\Gamma$. Under free evolution, for $\Gamma = 0$ we see coherent tunnelling from one well to the other. As the measurement parameter is increased

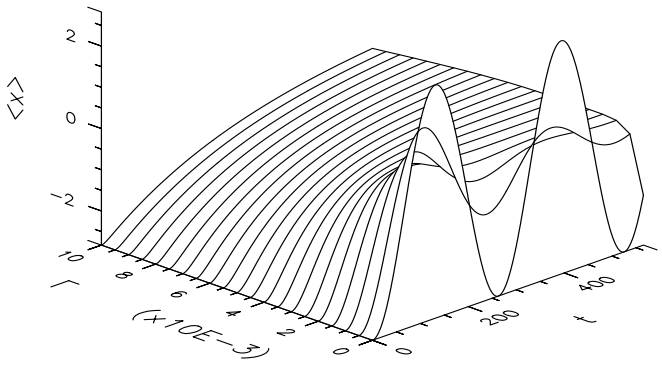


FIG. 7: Plot the non-selective evolution of the average value of position $\langle\hat{x}\rangle$ for a particle for various values of the measurement parameter $\Gamma$. As the measurement parameter increases the free oscillations of unitary evolution become increasingly damped. For very large $\Gamma$ the survival time of the particle in the left hand well is significantly enhanced, which is how the quantum Zeno effect is manifest in the non-selective case.

this unitary evolution is gradually damped. Indeed, for $8D\Gamma > \Delta$ oscillations cease, and the particle probability density gradually diffuses from the left well. For very large $\Gamma$ the survival time of the particle in the left hand well is enhanced due to the non-selective measurement. This is the non-selective quantum Zeno effect. Of course this result applies to the real particle only as long as we are able to successfully model the system with a discrete measurement basis.

In all nonselective measurement regimes $\Gamma > 0$ the particle will evolve to the long time mixed state $\rho_{NS}(\infty) = \frac{1}{2}\mathbf{I}$. Such a state can be considered as made up of an ensemble of selectively measured systems. For weak measurements each individual system is undergoing tunnelling with added noise due to the measurement backaction, as seen in Fig. 6(b). The effect of this noise is to cause different elements of the ensemble to become dephased. This is the origin of the damped oscillation seen in the nonselective (ensemble) evolution. In the strong measurement limit the measurement backaction dominates the evolution, causing the particle to act as a two state "random telegraph". This can be shown by considering the non-selective evolution of the system as above. In this case, we expect that the evolution is well described by rate equations with equal transition probabilities between the wells. That is, we should get an equation of the form

$$\dot{\hat{\rho}}_{11} = -\dot{\hat{\rho}}_{22} = -R\hat{\rho}_{11} + R\hat{\rho}_{22} \tag{42}$$

Now, in the limit of large $\Gamma$, Eq. (41) gives the following

$$Z(t) \approx -\frac{1}{/}2\exp\left(-\frac{\Delta^2}{16D\Gamma}t\right). \tag{43}$$

Since $Z = \frac{1}{2}(\rho_{22} - \rho_{11})$, we see that this equation is compatible to the rate equation [Eq. (42)] if we set the random telegraph transition rate to be

$$R = \frac{\Delta^2}{32D\Gamma} \tag{44}$$

This demonstrates the clearest possible manifestation of the quantum Zeno effect in that the transition probability is inversely proportional to the measurement parameter.

## IV. CONCLUSION

We have constructed a general model for the measurement interaction between a quantum system and single pseudo-classical meter. The meter is pseudo-classical in the sense that its mass is so large that it always has a well defined position and velocity. The system-meter interaction Hamiltonian is the usual von Neumann one. The meter state is measured innacurately at regular intervals. By carefully choosing the parameters, it is possible to take the limit of continuous measurements. Our central equation is a stochastic Schrödinger equation which describes the selective evolution of the system state under measurement. This equation conditions the system state on the measurement result, and tends to cause the system to collapse towards an eigenstate of the measured quantity. Feedback on the meter constrains it to behave as an ideal laboratory pointer, tracking the position of the system. It is the interpretation in terms of a realistic coupling to a single finite meter which we believe is new in this area.

The model is applied to monitoring the position of a particle in a double well potential. This system exhibits different behaviour depending on the relative strength of the measurement. The free particle tunnels coherently from one well to the other. With weak measurement, the tunnelling persists, but with diffusive noise added. This noise causes dephasing of the tunnelling within the ensemble of pure state trajectories, which leads to damped oscillations in the ensemble average (represented by a density operator). As the measurement becomes stronger, coherent tunnelling is replaced by incoherent flipping. This is a manifestation of the quantum Zeno effect, as the average time the particle remains stuck in its initial well increases approximately linearly with the measurement strength. This finding contradicts a recent claim by Fearn and Lamb[12] that there is no Zeno effect in a continuously monitored particle in a double well potential . The nonselective evolution in this case exhibits overdamping. For very strong measurements, the energy of the particle increases so quickly that it does not remain localized in either well for any significant length of time, and so the Zeno effect cannot be observed. We believe that it is this last type of behaviour which would always be produced by the measurement model of Lamb and Fearn, leading them to the wrong conclusion.

## APPENDIX A: NUMERICAL METHOD OF SIMULATION

In this appendix we describe the numerical method used for solution of the stochastic Schrödinger Eq. (19) in the double well. As long the particle is not to energetic, we can use a truncated basis to model the system. Rather than use the eigenstates of the Hamiltonian, we choose to work in the well known number state basis for a harmonic oscillator potential centred at the origin. Such states are complete and have the position representation of

$$\langle x|n\rangle = \pi^{-\frac{1}{4}}(2n!)^{-\frac{1}{2}}H_n(x)e^{-x^2/2}, \tag{A1}$$

where $H_n(x)$ is a Hermite polonomial. We transform to

the operators

$$\hat{x} \rightarrow \hat{X} = \frac{1}{\sqrt{2}}(a + a^\dagger)$$
$$\hat{p} \rightarrow \hat{Y} = -\frac{i}{\sqrt{2}}(a - a^\dagger), \qquad \text{(A2)}$$

with the appropriate transformations of the free Hamiltonian. The initial state of the particle is $|-\rangle$, which is localised in the left minimum of the double well potential. This state is readily calculated in the number state basis. For computational purposes we must eventually truncate our number state basis. The validity of this truncation can be immediately assessed by noting that the initial state is well approximated by a coherent state $|\alpha\rangle$ located at $\alpha \approx -2\sqrt{D}$. As usual, this state has a number state expansion peaked about the mean $\bar{n} \approx 4D = 4$. This suggests that a truncation of the number basis at about 40 would be adequate. In this case the problem is quite manageable on a computer.


[1] W. Pauli, *General Principles of Quantum Mechanics* Springer-Verlag, Berlin (1980)
[2] B. Misra and E. C. G. Sudarshan, J. Math. Phys., **18**, 756 (1977)
[3] A Peres, Am. J. Phys., **48**, 931 (1980)
[4] E. Joos, Phys. Rev. D, **29**, 1626 (1984)
[5] C. M. Caves, G. J. Milburn, Phys. Rev. A, **36**, 5543 (1987)
[6] W. E. Lamb, Jr., in *Quantum Measurement and Chaos*, edited by E. R. Pike and S. Sarkar (Plenum, New York, 1987)
[7] N. Gisin, Phys. Rev. Lett., **52**, 1657 (1984); **53**, 1776 (1984); Helv. Phys. Acta., **62**, 363 (1989)
[8] L. Diosi, Phys. Lett. A, **120**, 377 (1987); **129**, 419 (1988); **132**, 233 (1989)
[9] L. Diosi, Phys. Rev. A, **40**, 1165 (1989)
[10] P. Pearle, Phys. Rev. A, **39**, 2277 (1989)
[11] V. P. Belavkin, P. Staszewski, Phys. Rev. A, **45**, 1347 (1992)
[12] H. Fearn, W. E. Lamb, Jr., Phys. Rev. A, **46**, 1199 (1992)
[13] G. J. Milburn, J. Opt. Soc. Am. B, **5**, 1317 (1988)
[14] L. L. Bonilla, F. Guinea, Phys. Rev. A, **45**, 7718 (1992)
[15] J. von Neumann, "Mathematische Grundlagen der Quanten-mechanik", (Springer, Berlin, 1932), especially Chap. 6 [English translation: "Mathematical Foundations of Quantum Mechanics", (Princeton University , Princeton, New Jersey, 1955)]
[16] W. Heisenberg, "The Physical Principles of Quantum Mechanics", (The University of Chicago Press, Chicago, 1930)
[17] H. M. Wiseman, G. J. Milburn, Phys. Rev. A, **47**, 1652 (1993)
[18] N. Gisin, I. C. Percival, Phys. Lett. A, **167**, 315, (1992): J. Phys. A: Math. Gen., **25**, 5677 (1992)
[19] C. W. Gardiner, A. S. Parkins and P. Zoller, Phys. Rev. A, **46**, 4363 (1992)
[20] A. O. Caldeira, A. J. Leggett, Ann. Phys. (N. Y. ) **149**, 374 (1983), **153**, 445 (1983) (Erratum)
[21] A. J. Leggett, S. Chakravarti, A. T. Dorsey, M. P. A. Fisher, A. Garg, W. Zwerger, Rev. Mod. Phys., **59**, 1 (1987)
[22] F. Grossmann, P. Jung, T. Dittrich and P. Hänggi, Z. Phys. B, **84**, 315 (1991)